# MODELLING OF BINARY MIXTURE COMMINUTION

F. E. P. SUDÁRIO and J. A. M. LUZ

*Mining Eng. Department, Universidade Federal de Ouro Preto, Minas Gerais, Brazil.*
*flaviaemery@gmail.com*

***Abstract*— This paper treats on grindability differences of mineral mixtures to achieve a preliminary selective particle size contrast by comminution in order to improve further sorting operation. Quartz and calcite had been chosen as example of binary system. The theoretical basis for this work was inspired by the optimization study carried out by Ray and Szekely (1973), through an algebraic model based on evolution of log-normal distribution of particle size during comminution. On the other hand, the present work has described grindability differences through the classical Rosin-Rammler size distribution. The study of the evaluation of binary mixture differences was realized by sieving analyses and the estimation of Rosin-Rammler sharpness and median diameter. An objective function was conceived stressing the relationship between the expended energy in the grinding process and the optimum residence time. It is possible to use the results as a background for grinding optimization system, since that the penalty function inside objective function can be adequately calibrated as far as technical and economic impacts on further sorting separations are concerned.**

***Keywords*— grindability; granular media; Rosin-Rammler; unit operations.**

## I. INTRODUCTION

Currently, it is well known that the selection and break process of the particle in the comminution is obtained by impact breaking, compression and abrasion. Knowledge of the forces acting on particles in the different types of ores can contribute for the improvement of mineral processing. Several models were created to describe forces acting on the particles during the break process. The formalism that has been by far most used is the population balance (King, 2001; Beraldo, 1987).

The critical operation in the processing of minerals is sorting. For their achievement, it is usual to apply comminution to achieve the necessary liberation. Ores constituted of minerals displaying differences in hardness, cleavage, parting and grindability have possibilities of economic gain in a processing plant, by particle size differentiation of the species to be separated. Such an optimum size contrast between the two species meets the compromise among the following parameters: liberation degree, selective size difference of components, concentration efficiency and specific energy consumption.

Modeling of comminution usually is performed employing the population balance approach. This method is based in two stochastic functions: the selection function (linked to probability of each particle being selected in a single comminution event) and the breakage function, which quantifies the progeny's size distribution (Fuerstenau *et al.*, 2003; Beraldo, 1987). So the model can predict particle size distribution of product after comminution. Non linearities in model equations can jeopardize the accuracy of the simulation, as already pointed out by Aboukheshem *et al.* (1986) and Bilgili and Scarlett (2005). Alternatively, using Lagrange's multipliers method, Otwinowski (2006) has applied the maximum informational entropy to determine the breakage function.

Another interesting approach was used by Ray and Szekely (1973), who used a objective function based on maximization of the benefit that a selective comminution gives to the subsequent process with a penalty cost function for comminution. They used the difference between the mean sizes at the exit of the mill as quantification criterion for the benefit. These authors used the **discrete maximum principle** for optimization in systems of decomposed structure. The model is based in the population balance model obeying the log-normal distribution, which is described by:

$$y(d) = \frac{1}{\log\sigma\sqrt{2\pi}} \exp\left\{-\left[\frac{\left(\log d - \log \bar{d}\right)^2}{2\log^2\sigma}\right]\right\} \qquad (1)$$

where $\bar{d}$ is the median diameter of the particle; $\sigma^2$ is the variance of size distribution of the material; $y(d)$ is the fraction of material with diameters between $d$ and $d + \Delta d$. Modifying such an approach of mixture comminution modeling the present work has studied the behavior of an binary ore in the grinding process, using a synthetic quartz and calcite mixture. The theoretical results obtained by Ray and Szekely through the interaction of two materials of different grindability (said A and B) were found by using the log normal size distribution and linking the intersection area of the curves for material A and B with the possible separation capability of post-comminution equipment, associated to differences of mean sizes and standard deviations as discriminant parameters.

In parallel to this work Rosa and Luz (2010a; 2010b) had studied selective grinding of binary mixtures, aiming to simulate it by artificial neural network.

## II. METHODS

The behavior of a synthetic ore during grinding was studied using the evolution of the mean size and sharpness of the Rosin-Rammler-Sperling-Bennet distribution

as control. Isolated calcite and quartz were studied and also binary mixture with 20 %, 40 %, 60 %, and 80 % of calcite. Milling times were: 300 s, 900 s, 1800 s, 3600 s and 7200 s.

Firstly, all quartz and the calcite samples was previously crushed (separately) below 3.35 mm. Representative sample mass for grinding tests was calculated according to Gy's method (Wills and Napier-Munn, 2005).

Ball diameter was selected with aid of the Bond equation (Beraldo, 1987). The steel mill used was unlined and had the following dimensions: 200 mm diameter and 200 mm in length. The tests were conducted in batch and dry operation.

The mainly used software for curve fitting and statistical analysis was EasyPlot for Windows, version 4.0.4. Its algorithm uses a Marquardt-Levenberg filter, which, opposed the simplex search algorithm, allows the estimation of uncertainties associated with the values of regression (Luz, 2005). Fitting curves of the median diameter and the sharpness versus grinding time was obtained using FindGraph (software by UniPhiz Lab). Math derivation was done using the program Mathematica 7, that is a computer program for programming, mathematical modeling, simulation, data manipulation, graphical visualization, supporting several research areas, developed by Stephen Wolfram, Wolfram's. Algorithms were developed in Scilab.

Sieving tests were performed in duplicate for all samples. The experimental size data were input for statistical fitting of Rosin-Rammler curves using Easyplot. After the fitting process, sharpness and median diameter were used for simulating purposes. Behavioral analysis of calcite and quartz was carried out through the evolution of median diameter and the sharpness of the Rosin-Rammler distribution:

$$Y_i = 1 - \exp\left[\ln(0,5)\left(\frac{d_i}{d_{50}}\right)^m\right] \qquad (2)$$

where: $Y_i$ is the fraction of the material passing through size class i[-]; $d_i$ is the size (diameter) of class $\boldsymbol{i}$ [m]; $d_{50}$ is the median diameter of particle size distribution [m]; $m$ is the sharpness parameter [-]. The higher the sharpness, the narrower the range of the distribution is.

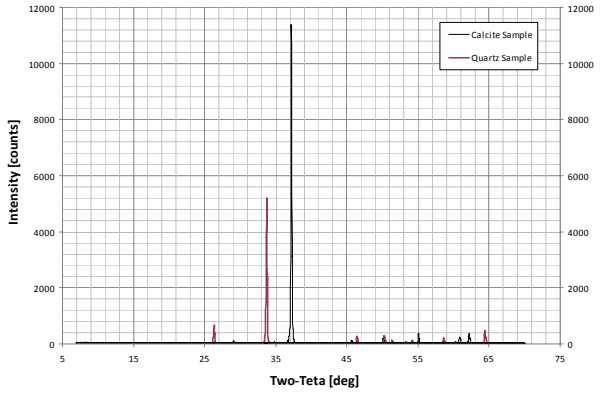


**Fig. 1:** Diffractograms of quartz and calcite.

Calcite content in the mixture in each size class was estimated by loss of ignition at 950 ºC (for 3,600 seconds). The weight loss corresponded to the evolution of $CO_2$, permits the stoichiometric calculation of the calcite content in the mixture.

X-ray diffraction analysis has confirmed the microstructure of quartz and calcite crystals. The two diffractograms met respectively the standard patterns for calcite and quartz (Fig. 1).

## III. RESULTS AND DISCUSSION

The interesting aspect in this work is the mutual influence of the proportion of quartz and calcite in the binary mixture, measured by the differences in size distribution, since the sharpness evolution of the mixture with grinding time showed the influence that a mineral does workout over the other one, as comparing with results obtained by grinding each one separately.

This work was completed with an objective function obtained through empirical and theoretical results which relates the intersection area of the curves of quartz and calcite with a penalty function depending on the (cost related) time of grinding.

The results of particle size analysis of each isolated material by Rosin-Rammler curve fitting are shown in Fig. 2 and 3 (whose experimental conditions are summarized in Tables 1, 2, 3 and 4).

The operational conditions and the symbols for curves of Fig. 2 are systematized in Table 1 and the conditions referring the Fig. 3 shown in Table 2.

The mutual influence of mineralogical species of the binary mixtures (calcite and quartz in proportion 60%:40% ; 40%:60%; 20%:80 %; and 80%:20 %) was studied and can be inferred from analysis of Figs. 4 to 7. The operating conditions and the symbols used for the curves of Fig. 4 are systematized in Table 3.

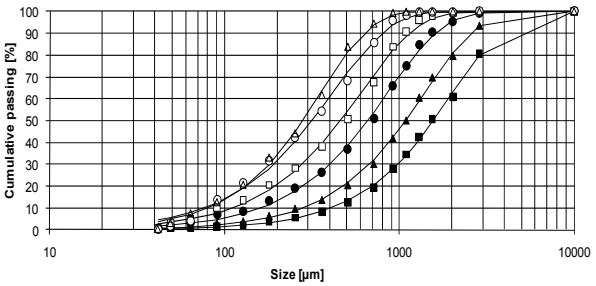


**Fig. 2:** Evolution of particle size distribution of isolated quartz with Rosin-Rammler regression.

**Table 1:** Distribution size evolution of quartz and the Rosin-Rammler curve (data of Fig. 2)

| Grinding time [s] | Sharpness | Median diameter [µm] | $R^2$ | Symbol in Figure 2 |
|---|---|---|---|---|
| 0 | 1.40 | 1568 | 0.999 | ■ |
| 300 | 1.40 | 1084 | 0.999 | ▲ |
| 900 | 1.35 | 658 | 0.998 | ● |
| 1800 | 1.33 | 463 | 0.997 | □ |
| 3600 | 1.31 | 319 | 0.996 | ○ |
| 7200 | 1.51 | 281 | 0.999 | △ |

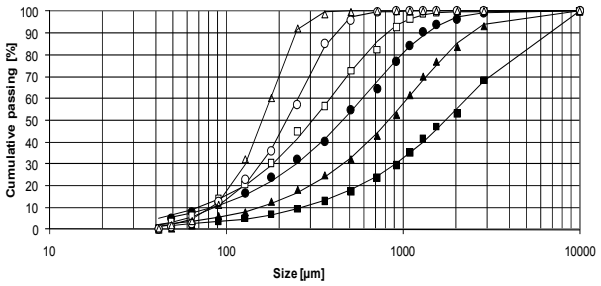


**Fig. 3:** Evolution of particle size distribution of isolated calcite with Rosin-Rammler regression.

**Table 2:** Distribution size evolution of calcite and the Rosin-Rammler curve (data of Figure 3).

| Grinding time [s] | Sharpness | Median diameter [µm] | $R^2$ | Symbol in Figure 3 |
|---|---|---|---|---|
| 0 | 1.01 | 1754 | 0.998 | ■ |
| 300 | 1.13 | 830 | 0.998 | ▲ |
| 900 | 1.10 | 458 | 0.998 | ● |
| 1800 | 1.26 | 312 | 0.997 | □ |
| 3600 | 2.00 | 223 | 0.999 | ○ |
| 7200 | 2.85 | 162 | 1.000 | △ |

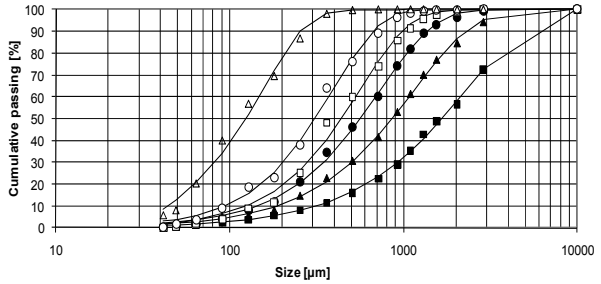


**Fig. 4:** Temporal evolution in the mixture of calcite (60 %) and quartz (40 %) with Rosin-Rammler regression.

**Table 3:** Distribution evolution of calcite (60 %) and quartz (40 %), and the Rosin-Rammler curve (data of Figure 4).

| Grinding time [s] | Sharpness | Median diameter [µm] | $R^2$ | Symbol in Figure 4 |
|---|---|---|---|---|
| 0 | 1.14 | 1659 | 0.998 | ■ |
| 300 | 1.24 | 858 | 0.999 | ▲ |
| 900 | 1.37 | 565 | 0.999 | ● |
| 1800 | 1.49 | 440 | 0.995 | □ |
| 3600 | 1.57 | 310 | 0.997 | ○ |
| 7200 | 1.64 | 174 | 0.994 | △ |

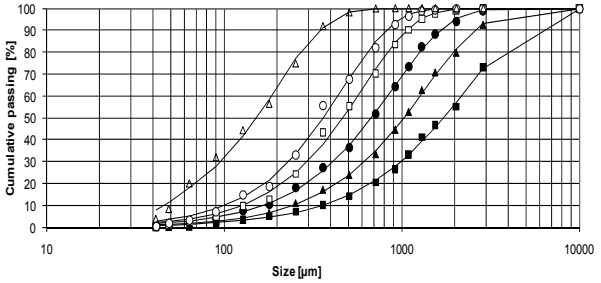


**Fig. 5:** Evolution of the global grain mixture of 40 % calcite and 60 % quartz with Rosin-Rammler regression (conditions and symbols are in Table 4).

**Table 4:** Distribution evolution of calcite (40 %) and quartz (60 %), and the Rosin-Rammler curve (data in Figure 5).

| Grinding time [s] | Sharpness | Median diameter [µm] | $R^2$ | Symbol in Figure 5 |
|---|---|---|---|---|
| 0 | 1.21 | 1721 | 0.998 | ■ |
| 300 | 1.32 | 1033 | 0.999 | ▲ |
| 900 | 1.35 | 679 | 0.999 | ● |
| 1800 | 1.45 | 468 | 0.998 | □ |
| 3600 | 1.49 | 364 | 0.997 | ○ |
| 7200 | 1.45 | 215 | 0.996 | △ |

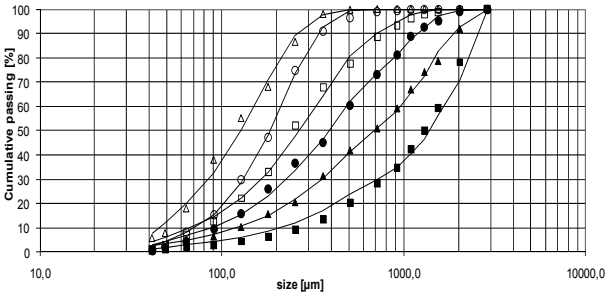


**Fig. 6:** Evolution of the global grain mixture of 80 % calcite and 20 % quartz with Rosin-Rammler regression (conditions and symbols are in Table 5).

**Table 5:** Distribution evolution of calcite (80 %) and quartz (20 %), and the Rosin-Rammler curve (in Figure 6).

| Grinding time [s] | Sharpness | Median diameter [µm] | $R^2$ | Symbol in Figure 6 |
|---|---|---|---|---|
| 0 | 1.08 | 1705 | 0.998 | ■ |
| 300 | 1.14 | 896 | 0.998 | ▲ |
| 900 | 1.27 | 549 | 0.997 | ● |
| 1800 | 1.37 | 379 | 0.997 | □ |
| 3600 | 1.99 | 260 | 0.999 | ○ |
| 7200 | 1.66 | 179 | 0.995 | △ |

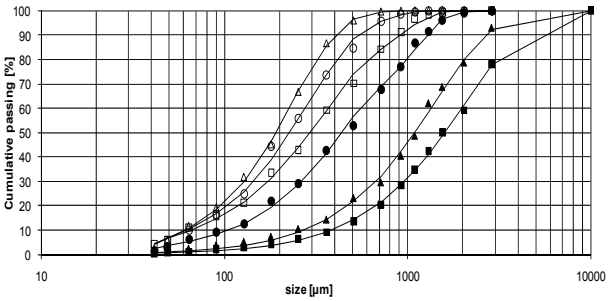


**Fig. 7:** Evolution of the global grain mixture of 20 % calcite and 80 % quartz with Rosin-Rammler regression (conditions and symbols are in Table 6).

**Table 6:** Distribution evolution of calcite (20 %) and quartz (80 %), and the Rosin-Rammler curve (data in Figure 7).

| Grinding time [s] | Sharpness | Median diameter [µm] | $R^2$ | Symbol in Figure 7 |
|---|---|---|---|---|
| 0 | 1.32 | 1596 | 0.999 | ■ |
| 300 | 1.36 | 1093 | 0.997 | ▲ |
| 900 | 1.32 | 619 | 0.998 | ● |
| 1800 | 1.25 | 418 | 0.998 | □ |
| 3600 | 1.44 | 323 | 0.997 | ○ |
| 7200 | 1.63 | 270 | 0.999 | △ |

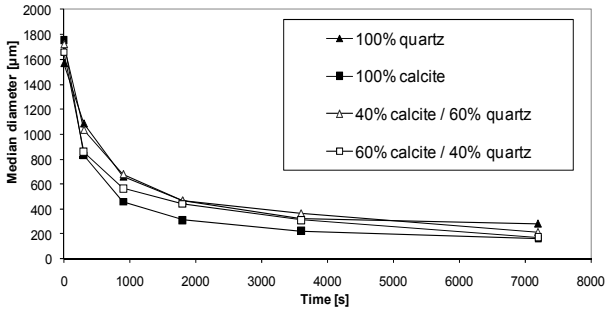


**Fig. 8:** Median diameter evolution of the mixture of 40 % and 60 % calcite and of the isolated quartz and isolated calcite.

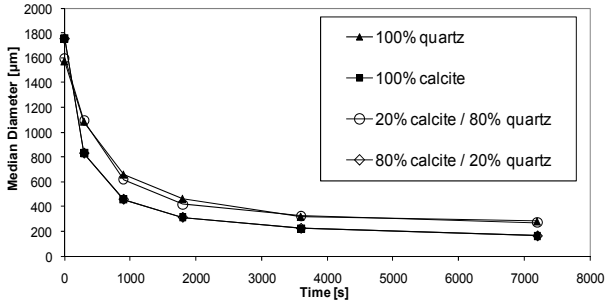


**Fig. 9;** Median diameter evolution of the mixture of 20 % and 80 % calcite and of the pure quartz and isolated calcite.

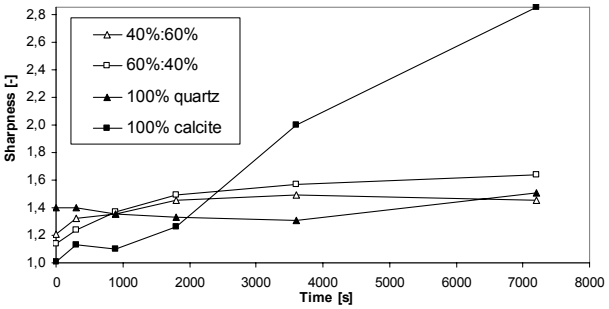


**Fig. 10:** Sharpness evolution for mixtures of 40 % and 60 % calcite and of the isolated quartz and isolated calcite.

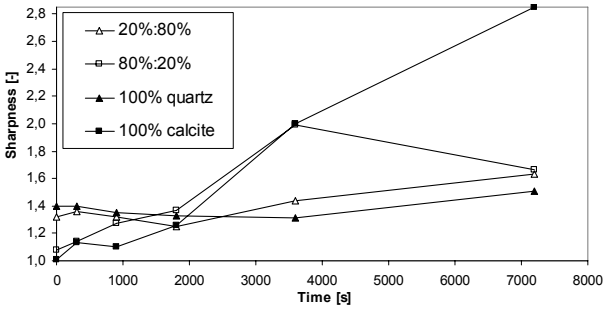


**Fig. 11:** Sharpness evolution for mixtures of 20 % and 80 % calcite and of the isolated quartz and isolated calcite.

Aiming the detection improvement of the composition effect on grindability of binary mixtures, the regression values corresponding to the average size ($d_{50}$) and the sharpness of the distribution of each mixture ($m$) were plotted in Figs. 8, 9, 10 and 11.

The evolution of median diameter, referring to the various mixtures studied is shown in graphs of Fig. 8 and 9. It is seen that there was typical behavior for the median diameter for comminution processes, since there was systematical decrease of graining with the increasing milling time. Note also, the typical behavior of asymptotic attenuation of the curve (fact well known in the industry).

According to the temporal evolution of sharpness in Rosin-Rammler distribution referred to the global mix, it can be seen in Fig. 10 and 3.11. It should be remembered that the parameter ***m*** (the sharpness) is a measure of dispersion (analogous to standard deviation), contrary to the median diameter, which is a measure of central tendency. It can be seen that isolated quartz and calcite behave differently. In the quartz there is a tendency to preserve the amplitude distribution with a slight decrease in sharpness and increasing milling time.

Pure calcite (which exhibits perfect cleavage) shows a great increase in sharpness with the milling time, showing the effect of preferential breakage of larger particles in a population initially with broader size distribution range.

In order to detect possible effects in the sharpness evolution of a mineral over the other one, it was also calculated a theoretical and hypothetical sharpness of the mixture, in case there were no mutual interference in the components of the mixture under comminution. This hypothetical sharpness was taken as the weighted average of values for the isolated minerals, having as weight factor the proportion of phases (calcite and quartz).

Figures 10 and 11 show the influence of the quartz in calcite grindability, when compared to isolated calcite, with the same milling time.

The comparison between hypothetical and experimental values are seen in Fig. 12 and 13. Fig. 10 and 11 show the difference in size distribution between quartz,

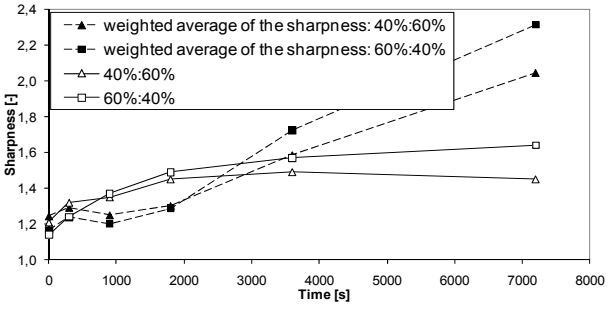


**Fig. 12:** Sharpness evolution of the simulated and real mixture for mixtures of 40 %:60 % calcite (solid squares).

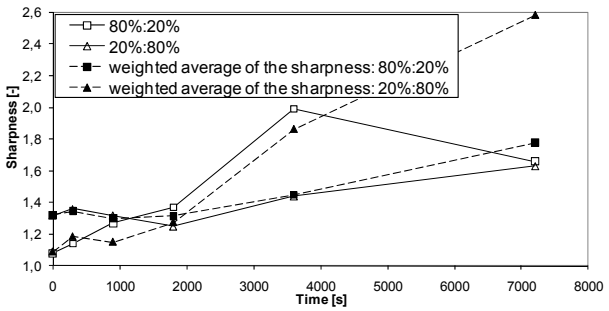


**Fig. 13:** Sharpness evolution of the simulated and real mixture for mixtures of 20 %:80 % calcite (solid squares).

**Table 7:** Relative deviation of the sharpness of the mixture distribution.

| Mixture of 40 % calcite and 60 % quartz | | | | Mixture of 60 % calcite and 40 % quartz | | |
|---|---|---|---|---|---|---|
| Time [s] | Experimental | Weighted | Relative deviation [%] | Experimental | Weighted | Relative deviation [%] |
| 0 | 1.21 | 1.24 | -2.81 | 1.14 | 1.17 | -2.28 |
| 300 | 1.32 | 1.29 | 2.12 | 1.24 | 1.24 | 0.16 |
| 900 | 1.35 | 1.25 | 7.41 | 1.37 | 1.20 | 12.41 |
| 1800 | 1.45 | 1.30 | 10.21 | 1.49 | 1.29 | 13.56 |
| 3600 | 1.49 | 1.59 | -6.44 | 1.57 | 1.72 | -9.81 |
| 7200 | 1.45 | 2.05 | -41.10 | 1.64 | 2.31 | -41.10 |

**Table 8:** Relative deviation of the sharpness in mixture distribution.

| Mixture of 20 % calcite and 80 % quartz | | | | Mixture of 80 % calcite and 20 % quartz | | |
|---|---|---|---|---|---|---|
| Time [s] | Experimental | Weighted | Relative deviation [%] | Experimental | Weighted | Relative deviation [%] |
| 0 | 1.20 | 1.32 | -9.47 | 1.09 | 1.09 | 0.18 |
| 300 | 1.36 | 1.35 | 1.03 | 1.14 | 1.18 | -3.86 |
| 900 | 1.32 | 1.30 | 1.52 | 1.27 | 1.15 | 9.45 |
| 1800 | 1.25 | 1.32 | -5.28 | 1.37 | 1.27 | 7.01 |
| 3600 | 1.44 | 1.45 | -0.56 | 1.99 | 1.86 | 6.43 |
| 7200 | 1.63 | 1.78 | -9.08 | 1.66 | 2.58 | -55.54 |

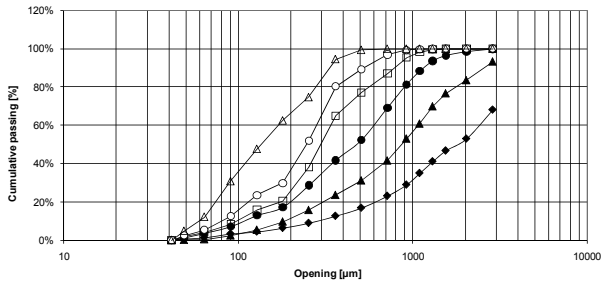


**Fig. 14:** Size distribution evolution of calcite in mixture calcite/quartz in proportion 40 % : 60 % (virtually isolated).

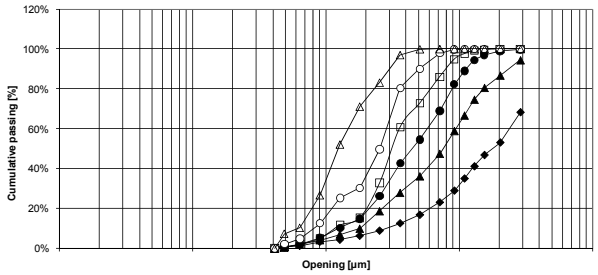


**Fig. 15:** Size distribution evolution of calcite in mixture calcite/quartz in proportion 60 % : 40 % (virtually isolated).

calcite and mixtures using values of sharpness parameter. The independence or not between quartz and calcite can also be evaluated by analyzing the sharpness parameter. Figures 12 and 13, show the curves that represent the condition for which the calcite and quartz behave independently during milling hypothetical, and the curves that represent the actual situation obtained by experiments.

Tables 7 and 8 show the relative deviations between empirical and hypothetical values (weighted average) of the sharpness in the mixtures. It can be seen clearly that there is interference, because the deviations are appreciable for larger grinding times. The first point of table 8 was aberrant, indicating experimental error. Anyway, as the relative deviations are appreciable, the hypothesis of no interference can be ruled out. The effects of mutual interference in the comminution of the two mineralogical species in mixture are more representative plotting the evolution of the two minerals separately. This is equivalent to consider when studying a given component that the other one would be part of the grinding media. The values of calcite and quartz sizes (virtually isolated) in function of grinding time are shown in Figs. 14, 15, 16 and 17.

Operational conditions for curves of Figs. 14 and 15 are in Tables 9 and 10, and operational conditions for curves of Figs. 16 and 17 are in Tables 11 and 12.

**A. Mathematical Model of the Size Distribution Contrast.**

Fitting was made according to the Rosin-Rammler curve (Eq. 3) in relation to the cumulative passing of all material. The form of the equation found for the median diameter in relation to the time from 0 to 7,200 seconds was:

$$y = a \times \exp\left(-\frac{t}{b}\right) + c \tag{3}$$

where, $t$ is time (seconds); $a$, $b$ e $c$ are constant.

The sharpness in relation to the time from 0 to 7,200 seconds was fitted to:

$$y = a \times t^3 + b \times t^2 + c \times t + d \tag{4}$$

where, t is time (seconds); $a$, $b$, $c$ and $d$ are constants.

**Table 9:** Composition effect on temporal evolution of median diameter.

| Calcite's median diameter Evolution (virtually isolated) | | | | Quartz's median diameter evolution (virtually isolated) | | | Symbol in Figures 14 and 15 |
|---|---|---|---|---|---|---|---|
| time [s] | 100 % (pure) [µm] | 60 % [µm] | 40 % [µm] | 100 % (pure) [µm] | 60 % [µm] | 40 % [µm] | |
| 0 | 1754 | 1769 | 1769 | 1568 | 1570 | 1570 | ■ |
| 300 | 830 | 748 | 858 | 1084 | 1154 | 1041 | ▲ |
| 900 | 458 | 456 | 467 | 658 | 849 | 727 | ● |
| 1800 | 312 | 346 | 315 | 463 | 594 | 614 | □ |
| 3600 | 223 | 242 | 243 | 319 | 471 | 447 | ○ |
| 7200 | 162 | 150 | 137 | 278 | 286 | 253 | △ |

**Table 10:** Composition and temporal evolution of sharpness, *m*.

| Calcite's sharpness evolution (virtually isolated) | | | | Quartz's sharpness evolution (virtually isolated) | | | Symbol in Figures 14 and 15 |
|---|---|---|---|---|---|---|---|
| Time [s] | 40% | 100 % (pure) | 60 % | 40 % | 100% (pure) | 60 % | |
| 0 | 1.04 | 1.01 | 1.04 | 1.04 | 1.40 | 1.43 | ■ |
| 300 | 1.20 | 1.13 | 1.18 | 1.20 | 1.40 | 1.45 | ▲ |
| 900 | 1.30 | 1.10 | 1.39 | 1.30 | 1.35 | 1.54 | ● |
| 1800 | 1.60 | 1.26 | 1.71 | 1.60 | 1.33 | 1.64 | □ |
| 3600 | 1.77 | 2.00 | 1.79 | 1.77 | 1.31 | 1.65 | ○ |
| 7200 | 2.85 | 1.95 | 1.66 | 1.51 | 1.66 | 1.84 | △ |

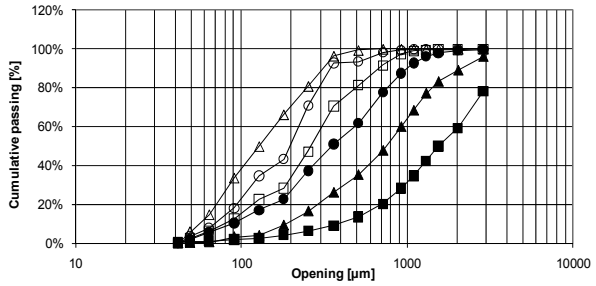


**Fig. 16:** Size distribution evolution of calcite in mixture calcite/quartz in proportion 20 % : 80 %.

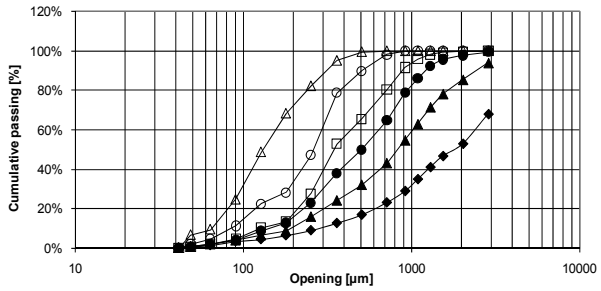


**Fig. 17:** Size distribution evolution of calcite in mixture calcite/quartz in proportion 80 % : 20 %.

**Table 11:** Composition and evolution of diameter.

| Calcite's median diameter Evolution (virtually isolated) | | | | Quartz's median diameter evolution (virtually isolated) | | | Symbol in Figures 16 and 17 |
|---|---|---|---|---|---|---|---|
| tempo [s] | 100 % (pure) [µm] | 20 % [µm] | 80 % [µm] | 100 % (pure) [µm] | 20 % [µm] | 80 % [µm] | |
| 0 | 1754 | 1769 | 1769 | 1568 | 1570 | 1570 | ■ |
| 300 | 830 | 747 | 826 | 1084 | 993 | 1106 | ▲ |
| 900 | 458 | 377 | 499 | 568 | 768 | 766 | ● |
| 1800 | 312 | 270 | 394 | 463 | 611 | 521 | □ |
| 3600 | 223 | 186 | 252 | 319 | 521 | 411 | ○ |
| 7200 | 162 | 139 | 143 | 278 | 285 | 251 | △ |

**Table 12:** Composition effect on evolution of sharpness, *m*.

| Calcite's sharpness Evolution (virtually isolated) | | | | Quartz's sharpness evolution (virtually isolated) | | | Symbol in Figures 16 and 17 |
|---|---|---|---|---|---|---|---|
| tempo [s] | 100 % (pure) | 20 % | 80 % | 100 % (pure) | 20 % | 80 % | |
| 0 | 1.01 | 1.04 | 1.04 | 1.40 | 1.43 | 1.43 | ■ |
| 300 | 1.13 | 1.29 | 1.21 | 1.40 | 1.33 | 1.37 | ▲ |
| 900 | 1.10 | 1.26 | 1.38 | 1.35 | 1.36 | 1.47 | ● |
| 1800 | 1.26 | 1.51 | 1.60 | 1.33 | 1.43 | 1.53 | □ |
| 3600 | 2.00 | 1.85 | 1.88 | 1.31 | 1.79 | 1.61 | ○ |
| 7200 | 2.85 | 1.72 | 1.92 | 1.51 | 2.01 | 1.54 | △ |

In order to quantify (in specific grinding time) the particle size contrast between the components, it is convenient to express this contrast in terms of intersection area between the two size distribution curves (Fig. 18).

The intersection (***I***) between the fitted Rosin-Rammler curves of calcite and quartz (Fig. 18) can be obtained by analytical procedure. The values of sharpness and the median diameter in relation to the time were found by the fitting curve shown in the Eqs. 3 and 4.

Such equations were incorporated into the Rosin-Rammler probability density equation:

$$f = \frac{m}{x_0} \times \left(\frac{x}{x_0}\right)^{m-1} \times \exp\left[-\left(\frac{x}{x_0}\right)^{m}\right] \quad (5)$$

The scale parameter ($x_0$) is obtained by the relationship:

$$x_0 = \frac{x_{50}}{\left[-\ln\left(\frac{1}{2}\right)\right]^{\frac{1}{m}}} \quad (6)$$

Considering the curve $f_A$ in the Figure 3.17 as being calcite and $f_B$ as the quartz curve, in the intersection one has:

$$f_A(x_I, y_I) - f_B\ (x_I, y_I) = 0 \quad (7)$$

The roots of this equation provide, naturally the intersection points of curves of the two components in the mixture in comminution, which are the coordinates $x_I$ and $y_I$. Equation 7 can be expressed by:

$$y = \frac{m_A}{x_{0A}} \times \left(\frac{x_I}{x_{0A}}\right)^{m_A-1} \times \exp\left[-\left(\frac{x_I}{x_{0A}}\right)^{m_A}\right] - \frac{m_B}{x_{0B}} \times \left(\frac{x_I}{x_{0B}}\right)^{m_B-1} \times \exp\left[-\left(\frac{x_I}{x_{0B}}\right)^{m_B}\right] = 0 \quad (8)$$

To implement the mathematical model, it was made the Newton-Raphson algorithm in Scilab for time from 0 to 7,200 seconds, with span of 10 seconds. Through this algorithm it was found the intersection values between the Rosin Rammler probability density equation of quartz and calcite. As Newton-Raphson method requires derivation of eq. 8, this was done using the program Mathematica 7, generating the following expression:

$$f'(x) = f_1'(x) + f_2'(x) + f_3'(x) + f_4'(x) \quad (9)$$

Being:

$$f_1'(x) = \frac{e^{-\left(\frac{x}{x_A}\right)^{ma}} \times \left(-1 + m_A\right) \times m_A \times \left(\frac{x}{x_A}\right)^{-2+m_A}}{x_A^{\,2}}$$

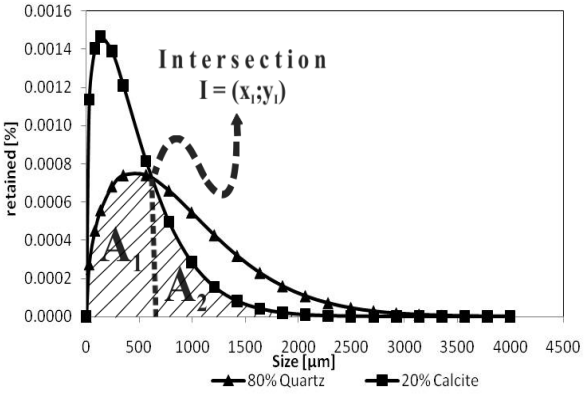


**Fig. 18:** Intersection point between the curves of the material A (calcite) and B (quartz) in a specific time coordinate (after beginning at t = 0).

$$f_2'(x) = -\frac{e^{-\left(\frac{x}{x_A}\right)^{m_A}} \times {m_A}^2 \times \left(\frac{x}{x_A}\right)^{-2+2\times m_A}}{{x_A}^2}$$

$$f_3'(x) = -\frac{e^{-\left(\frac{x}{x_B}\right)^{m_B}} \times \left(-1+m_B\right) \times m_B \times \left(\frac{x}{x_B}\right)^{-2+m_B}}{{x_B}^2}$$

$$f_4'(x) \frac{e^{-\left(\frac{x}{x_B}\right)^{m_B}} \times {m_B}^2 \times \left(\frac{x}{x_B}\right)^{-2+2\times m_B}}{{x_B}^2}$$

Newton-Raphson algorithm to find intersection values between the Rosin-Rammler density equation of quartz and calcite was made in Scilab, for 0 s to 7,200 s (time span of 10 seconds). After finding the value $I = (x_I;y_I)$, the calculation of the areas *A1* and *A2* can be done using the Rosin-Rammler cumulative distribution (integral), resulting the equation:

$$\text{Area A}_2 = 1 - Y_A\left(x = x_i\right) = 1 - \exp\left[-\left(\frac{x_I}{x_{0A}}\right)^{m_A}\right] \quad (10)$$

$$\text{Area A}_1 = Y_B\left(x = x_i\right) = \exp\left[-\left(\frac{x_I}{x_{0B}}\right)^{m_B}\right] \quad (11)$$

The following expression is shown as an example of final expression for the areas calculation, and refers to the calculation of area $A_2$ for the mixture with 20% calcite, in a generic time interval, *t*:

$$Y_A\left(x = x_i\right) = \exp\left[-\left(\frac{x_I}{x_{0A}}\right)^{m}\right] \quad (12)$$

being:

$$m = -4{,}17e^{-12}t^3 + 1{,}18e^{-8}t^2 + 2{,}16e^{-4}t + 1{,}11 \quad (13)$$

$$d_{50} = 1544 \times \exp\left(-\frac{t}{300}\right) + 216 \quad (14)$$

$$x_{0A} = \frac{d_{50}}{\left[-\ln\left(\frac{1}{2}\right)\right]^{\frac{1}{m}}} \quad (15)$$

The objective function is then the sum of plot areas plus the cost weighted function, formed by multiplying a weight penalty function dependent (in a first approach), only of the operation cost.

$$f_{ob}^{(j)} = Minimize[(A_1 + A_2) + p \times f(\mathrm{c})] \quad (16)$$

where *p* is the weight factor and *f(c)* is the penalty function, encompassing the cost which is especially dependent of the grinding time, since with increasing grinding time, results increased energy spending. Parameter *p* also depends on the economical benefit resulting on the subsequent sorting operations. In each concrete and actual case this positive impact must be quantified usually by pilot scale testwork.

For grinding time, *t*, one has, after including the classical Bond's comminution equation:

$$f(c) = f(E,\$) = q \times Q \times 10 \times Wi \times \left(\frac{1}{\sqrt{P_{80}}} - \frac{1}{\sqrt{F_{80}}}\right) \times \mathrm{t} \quad (17)$$

where *Q* is the mass flowrate and *q* takes on account the other operational expenditures like grinding media and liners consumption, and so on (q>1).

The parameters: *Wi*, $F_{80}$ and $P_{80}$ of the previous equation are Bond's work index, screen openings which pass 80 % of the feed and 80 % of the product respectively.

## IV. CONCLUSIONS

With Rosin-Rammler equation one can detect difference between quartz and calcite with grinding time. The median diameter evolves according to negative exponential law, and no sensible impact on the composition of the mixture in this parameter was seen, as the size distributions of the two isolated minerals are concerned. The grinding progress did not affect significantly the sharpness parameter for quartz. The behavior of calcite, however, shows that the progress of grinding leads to a increase in amplitude of particle size distribution.

The interdependence of the behavior of the two minerals can be verified. The quartz presence during grinding of calcite led to increased sharpness parameter of calcite size distribution. This behavior is consistent with the fact that the calcite presents perfect rhombohedral cleavage, and lower hardness and strength as compared to quartz.

The results were promising to help decrease the cost of grinding and better sorting performance.

## REFERENCES


Aboukheshem, M, K. Prisbrey, L.R. Bunnell and J.M. Lytle, "Fourier shape descriptors and particle breakage energy," *Particulate Science and Technology*, **4,** 143 – 149 (1986).

Beraldo, J.L., *Moagem de Minérios em Moinhos Tubulares,* Edgard Blücher, São Paulo (1987).

Bilgili, E. and B. Scarlett, "Population balance modeling of non-linear effects in milling processes," *Powder Technology*, **153**, 59–71 (2005).

Fuerstenau, D.W., P.C. Kapur and A. De, "Modeling Breakage Kinetics in Various Dry Comminution Systems," *KONA,* **21,** 121 -132 (2003).

King, R.P, *Modeling & Simulation of Mineral Processing Systems,* Butterworth-Heinnemann (2001).

Luz, J.A.M., "Conversibilidade entre distribuições probabilísticas usadas em modelos de hidrociclones," *Revista Escola de Minas,* **58,** 89-93 (2005).

Otwinowski, H., "Maximum entropy method in comminution modeling," *Granular Matter,* **8**, 239–249 (2006).

Ray, W.H. and J. Szekely, *Process optimization, with applications in metallurgy and chemical engineering,* Wiley, New York (1973).

Rosa, G.M and J.A.M. Luz, "Seletividade na cominuição de mesclas de dolomita e quartzo," *Revista Escola de Minas*, **63** (2010).

Rosa, G.M. and J.A.M. Luz, "Dry Grinding of Dolomite and Quartz and its Simulation by a Neural Network," *XII$^{th}$ International Mineral Processing Symposium* (2010).

Wills, B.A. and T. Napier-Munn, *Mineral Processing Technology,* B-H Elsevier, Amsterdam (2005).

**Received: August 24, 2010.**
**Accepted: July 5, 2011.**
**Recommended by Subject Editor Orlando Alfano.**